Predicting Additive Manufacturing Build Cracks Using XFEM

Vishal Savane
(Dassault Systèmes SIMULIA Corp., Pune, India);

Jing Bi, Zhen-zhong Du, Victor Oancea
(Dassault Systèmes SIMULIA Corp., Johnston, RI, USA);

John Laureto
(Renishaw Inc., Greater Chicago, USA)

Abstract

Laser powder bed fusion additive manufacturing (LPBF-AM) technology is nowadays being used for complex, near net shape in service metal parts in various industries like aerospace, defense and automotive. While manufacturing such parts, users strive to choose the best print orientation considering build stability and minimizing support structure. Although support structures provide stiffness to the build and facilitate heat transfer from part to build plate, adapting support structures reduces the benefits of LPBF-AM in that it increases build time, manufacturing cost and can adversely affect the surface finish of a part. The biggest concern amongst all is that residual stresses are shown to fracture support structures leading to further exaggerated part distortion. It is therefore essential to understand how support strategy affects the build quality and design intelligent supports with added values such as heat sinks, fixtures and datums instead of thoughtless secondary supports.

In this paper, a first stage high pressure turbine is built using a hybrid support structure including solid and column supports. Column supports are designed with a reduced cross-sectional area when they come into contact with overhanging part regions for easy removal during post processing and to reduce stress build up. The LPBF-AM printer is used to print this turbine blade with a designed support strategy and the Finite Element Method (FEM) is used to simulate the print process to check distortion, structural integrity and residual stress. The Extended Finite Element Method (XFEM) which can simulate the crack initiation and propagation along an arbitrary, solution dependent path has been enhanced to support Additive Manufacturing process simulation and is used to model potential build cracks during the LPBF-AM process. First order tetrahedron elements are enriched to model the turbine blade and first order brick elements are enriched to model the support structures. A stress based criterion is used to determine crack initiation, followed by crack evolution governed by critical fracture energy, leading to eventual failure in the enriched elements. Build cracks are observed at the junction between the turbine blade and its column supports both in physical

print and in simulation. The results show that finite element simulations effectively capture the physics involved with the LPBF-AM process and accurately predict not only distortion and residual stresses but also support structure crack mechanisms and part separation from support during print. The simulation result is then used to guide the development of improved support strategy.

1.   Introduction

In the past decade, additive manufacturing (AM) made its way among revolutionary next generation technologies and had been widely used for prototyping. In the past few years, certain processes such as metal powder bed processes have gained popularity in the aerospace, medical, electronics and automobile industries for its remarkable freedom to create light weight organic and intricate shaped parts and support for industrial graded materials. In Laser Powder Bed Fusion Additive Manufacturing (LPBF-AM) process, parts are produced in a layer-by-layer fashion by spreading powder on metal bed and fusing it with laser or electron beam, turning CAD files directly into finished products or near net shape components without the need for expensive tooling or fixture. LPBF-AM is a viable option for the manufacturing of pressure blades for aero engine and power turbines [1]. Like any manufacturing process, AM technologies come with both unique capabilities and limitations. The printability of a part is dependent on part size and geometry, material type, slicing thickness, build orientation, support structure design, thermal conditions etc. Build orientation is a crucial parameter since it will affect the print tolerance, energy expended, and the volume of support structures required [2]. Build direction for any additive layer manufacturing is always defined as being in the Z axis - i.e. vertically from the build plate. Users strive to choose the correct build orientation to produce the most stable build with minimal support structure required. Support structures are an integral part of this process as shapes are built bottom up layer by layer. As the current layer is melted, it relies on the layers below it to provide both physical support and a heat conduction pathway. Overhang regions require support structures below. The justification for incorporating support structure in AM process can be summarized as:

•   Support structure acts as both path length to conduct heat to the build plate as well as rigidity enhancer to reduce the development of part distortion and residual stresses;

•   Support structures act as fixtures typically when fabricating unbalanced parts or the raw material (powder) is unable to sustain the weight of that part [3].

Along with these advantages, support structure introduces a few challenges. For example, the removal of support structures requires a significant amount of

manual work which adds extra post-processing steps such as cut, ground or mill operations after printing. These structures also increase the build time, adds to the cost of powder material and tend to cause poor surface finish. In most undesirable cases, with improper support strategies, support structures crack during the print, separate from the part and maximize part distortions that could render the part unusable. As LPBF-AM involves rapid heating and cooling, residual stresses are inherent to the process due to the large thermal gradients (e.x. 400°F to 3000°F). While additional layers on top of layers the residual stresses accumulate and build up resulting in distortion of the part/build. These can be disruptive when the support structure breaks leading to part pull away from support and curl up at the edges. Cracks induced and propagated through part in such high temperature gradient process is shown in Figure 1.
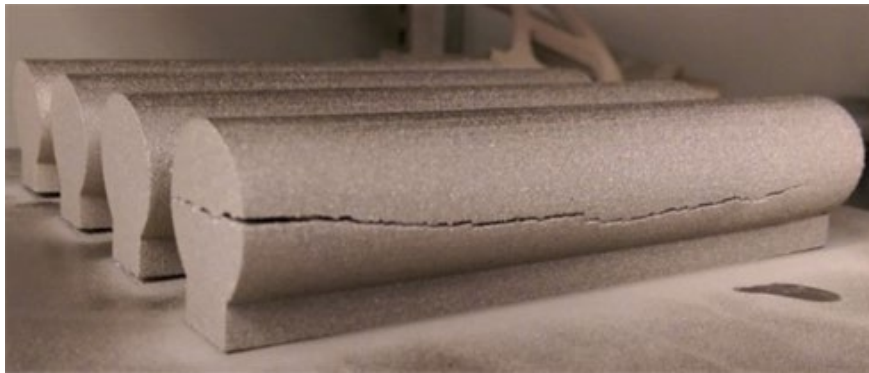
Figure 1:   Cracks induced in parts.

2.   Support Structure Design

Though support structure introduces challenges in LPBF-AM process, they are important as well for realizing a successful build. There is various literature that has been published on support structure design and its optimization. Minimizing/reducing need for support can be broadly achieved through keeping the original design intact or redesigning original design [3]. Methods, like choosing optimum part orientation, optimizing support structure through topology optimization or using lattice structure, are viable means to minimize support materials while keeping original design intact. Redesigning original part through topology optimization to minimize the area that requires supports below it or other methods like increasing overhang angles and redesigning features to be accommodating to the layer-based manufacturing method.

Support structures can be designed as primary and secondary supports [4]. Primary supports are those which are designed in the computer aided design (CAD) environment along with the component design and planned as sacrificial structures that will be removed once the build is finished. Secondary supports are those that are generated in machine build preparation software.

Secondary supports created within the build preparation software can also be managed via parameters, however lack parametric design control (i.e. they may need to be recreated if the part design or geometry orientation is modified). To obtain intelligent support solutions, one must take advantage of both the CAD system and the machine build preparation software. Primary value-added supports can work as heat sinks, fixtures, and datums. They can also be designed to work together with secondary supports to ease the support removal process after the print. Column supports can be designed to have a conical cross section at interface regions of the part to assist easy removal. Figure 2 shows the conical cross sectioned designs of column support(s).
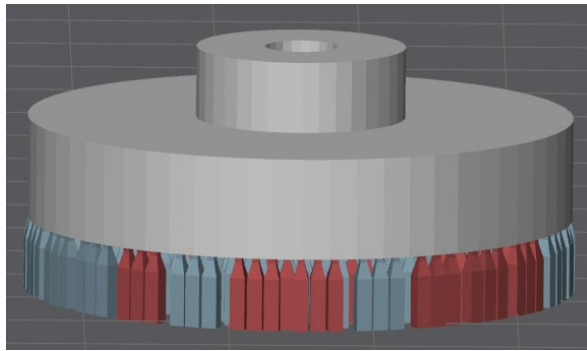

Figure 2:   Conical column supports in QuantAM v. 5.0.0.135

3.   Process Simulation Methodology

Three key components were developed to enable LPBF-AM process simulation that tracks crack initiation and propagation during the print process.

First, we use the Powder Bed Fabrication application on the **3D**EXPERIENCE platform that was developed to simulate the planning steps such as orienting the part properly on the build tray, nesting all parts that will be included in the build, generating support structures, generating scan paths and exporting this information to use in LPBF-AM printer [5]. Primary supports which are designed along with part CAD are imported and secondary supports can be generated on top of it. Scan paths are generated based on process parameters like laser power (W), hatch rotation angle (deg.), scan speed (m/s), layer thickness (μm), exposure time (μs) and scanning strategy. Figure 3 shows a scan path at one of the layers (red lines) for a Joiner model. The scan path information can then either be sent directly to the printer via a Virtual machine or neutral file formats, in this case, it is used as inputs for process simulations.
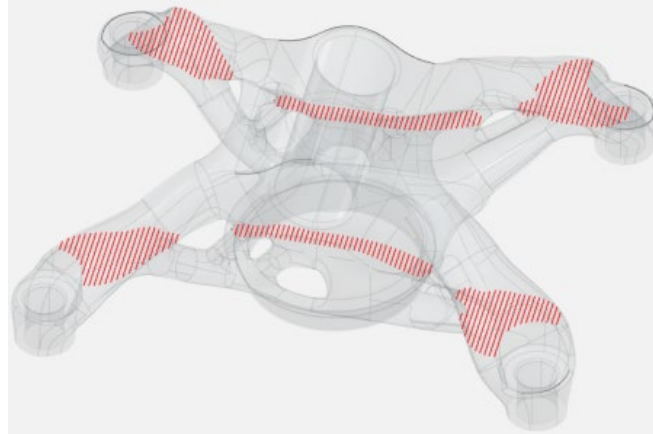
Figure 3:   Scan path for Joiner model

Being able to simulate the build planning steps together in the same environment as the part design is crucial because the additive manufacturing process forces designers and manufacturers to work more in collaboration. In addition to the laser processing parameters, as stated prior, the as-built component quality, yield, metallurgical integrity and dimensional conformity is highly dependent upon the LPBF-AM process parameters. Moreover, LPBF-AM processes will induce design constraints as result of laser beam waist (mm) minimums (i.e. minimum feature size) in conjunction with non-consolidated properties of the metal powder material. If a part has been designed for a fixed print orientation the build layout should not be changed prior to production processes. This information should be stored with the part and a machine programmer should be able to retrieve it during the build planning stage.

Similarly, LPBF-AM process planning is also carried out in QuantAM v5.0.0.135 where part and primary support imported in *.stl file format [6]. This file format uses a triangulated surface mesh to represent a 3D object. It is widely supported by many CAD packages, enabling model files to be easily exported or saved while providing user finite control of the surface mesh resolution. Build preparation stages like model positioning and alignment, support structures generation, slicing and scan path generation are carried out so that these settings can be exported to machine- readable format allowing manufacture using laser energy to melt fine metal powder on the LBPF-AM machines or continue to be used in subsequent realistic process simulations.

The second essential piece of the methodology is the process simulation framework. We have developed a general-purpose process simulation framework to support different types of thermomechanical additive manufacturing processes using data generated in the first stage [7].

The framework allows simulation of different additive manufacturing processes by representing material addition and energy addition events

separately in space and time. This is done mainly by the development of two modules: the mesh-intersection module and the moving heat flux module.

The mesh-intersection module allows the simulation to take machine tool path information in the form of time, location and field data and intersect the tool path data with any arbitrary mesh. The solver sweeps through of the finite element mesh by the tool path data and this intersection of mesh and tool path can be with the original part shape or with the deformed shape of the part. The tool path can be assigned with different geometric shapes as well (Figure 4). For example, in a LPBF-AM process, the laser is represented by a point and the wiper by an infinite line. For a polymer extrusion process, the nozzle path is represented as a rectangle.
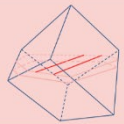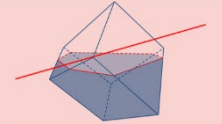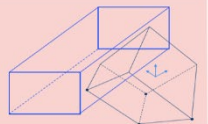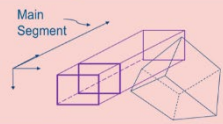
Shape	Point	Infinite Line	Rectangle	Box
Schematic				
Mesh intersection				Main Segment
Example	Point lasers for coarse meshes	Recoater in Powder Bed Fabrication	Material addition in polymer extrusion	Complex heating models (e.g.,Goldak)

Figure 4:   Different geometric shapes for tool path

In this simulation framework, Finite elements are activated in a progressive fashion during the analysis in a computationally efficient manner. During the simulation, any element could be completely or partially filled with material or empty. The solver precisely keeps track of this evolution, monitoring mass inventory and distribution to account for the addition of material during printing. The moving heat flux module was also developed to handle single/multiple moving heat sources of different shapes. Element external facets are computed as the material is being activated and this allows for a very precise assessment of cooling, regardless of the finite element discretization. Radiation and convection can be modeled on a continuously evolving surface that reflects the current shape of the part at any given point in the build.

At last, we enhanced the current XFEM technology so that it can be used for LPBF-AM process simulations. For example, the modelling of the crack susceptibility in nickel based super alloys. Modeling of such cracks as an enriched feature is commonly referred to as the extended finite element method (XFEM) which is an extension of the conventional finite element method based on the concept of partition of unity [8]. XFEM allows the presence of discontinuities in an element by enriching degrees of freedom with special displacement functions or additional phantom nodes without the requirement of

remeshing. XFEM based cohesive segments method is used to predict the crack initiation and propagation along an arbitrary, solution-dependent path in both the turbine blade and the support structures in this study.

4.   Aero Engine Turbine Blade

Aero engine power turbine blades are usually manufactured in nickel-base superalloys due to extreme heat during service [1]. These superalloys are more vulnerable to generating cracks because of their low thermal conductivity and high thermal expansion coefficient. [9]. Hot cracking may have a detrimental effect on the performance of structural components, especially during cyclic loading [10]. Typical defects found in LPBF-AM builds are microcracks, lack of fusion, pores and unwanted phases, such as oxides and inclusions. Cracking occurs when strain exceeds the materials ability to deform [11]. The high-temperature gradient combined with the residual stress causes the crack initiation and propagation within the fabricated part [12]. In the rest of this paper, we focus on the validation of the methodology on a realistic turbine blade part against experiment.

5.   Finite Element Modelling of Turbine Blade Printing Process

Initially, a first stage high-pressure turbine is considered in this study to be manufactured with LPBF-AM. As shown in Figure 5a, the turbine blade consists of a dovetail, a blade, and a shroud. To avoid the use of supports in blade region, the part is planned to be printed at a 45° orientation.
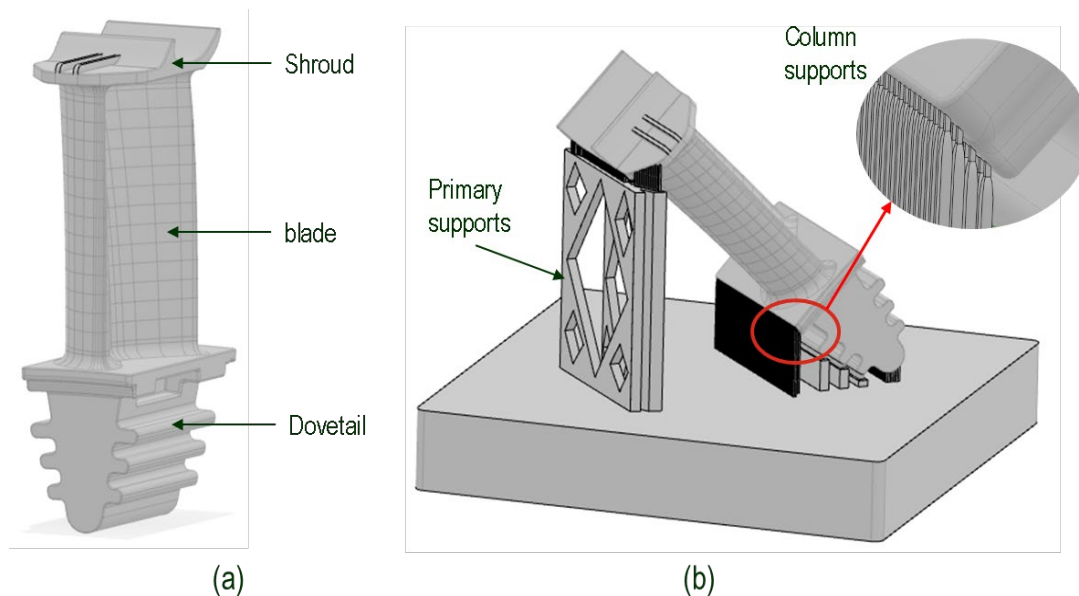

Figure 5:   (a) Turbine blade and (b) Build setup with intelligent support

For minimum material waste, the primary supports are designed to have diamond shaped pockets as shown in Figure 5b. Secondary column supports which connects between the primary supports and turbine blade as highlighted in red region in Figure 5b are designed with a conical cross section at conjunctions with the turbine blade part for easy support removal after print. Once the build setup is completed, process parameters are selected as shown in Table 1 and the scan path is generated using a strip strategy. Inconel 625 is selected as the printing material because of its nonmagnetic, corrosion and oxidation-resistant, excellent fatigue strength and stress-corrosion cracking resistance to chloride ions.

Table 1:   Process parameters

No.	Parameter	Values
1	Laser power	170 W
2	Layer thickness	60 μm
3	The angle of rotation between hatches	67°
4	Stripe width	5 mm
5	Hatching distance	140 μm

The sequentially coupled thermal mechanical analysis is performed in Abaqus/Standard [13] to predict temperature, distortion, residual stresses, possible crack initiation, and propagation during the print. Heat transfer analysis provides the temperature history of the process, which then drives the subsequent static analysis and the distortion, stress and cracks calculations. In this model, first order tetrahedron elements are used to mesh the turbine blade and primary supports whereas hexagonal elements are used for the secondary column supports. Mesh size convergence study is carried out to determine the proper mesh size to be used. Generated tool path in the format of time, location and field data is used to derive the material/element activation and heat addition. Only a small number of additional process parameters are necessary to complete the setup of the FE simulation (Table 2).

Table 2:   Simulation parameters

No.	Parameter	Values
1	Build tray dimension	248x248x33mm
2	Build substrate temperature	170°C
3	Wiper time	8sec
4	Absorption coeff	0.45
5	Convection coeff	18W/m^2K

XFEM based cohesive segments method in conjunction with the phantom nodes is used in this study. Such a method can be used to simulate crack initiation and propagation along an arbitrary, solution-dependent path in the bulk materials since the crack propagation is not tied to the element boundaries

in a mesh. Phantom nodes, which are superposed on the original real nodes, are introduced to represent the discontinuity of the cracked elements. When the element is intact, each phantom node is completely constrained to its corresponding real node. When the element is cut through by a crack, the cracked element splits into two parts. Each part is formed by a combination of some real and phantom nodes depending on the orientation of the crack. Each phantom node and its corresponding real node are no longer tied together and can move apart from each other. The separation of the phantom node and its corresponding nodes are governed by the cohesive traction-separation law until the fracture energy dissipated is equal to the critical value specified, after which the phantom node can move freely independently of the corresponding real node.

There are various criteria to model crack initiation like maximum principal stress/strain, maximum nominal stress/strain, quadratic traction-interaction, quadratic separation-interaction criterion, and user-defined damage initiation criterion. In this paper, we are using maximum principal stress criterion to determine the crack initiation at the turbine blade and the quadratic nominal stress criterion to determine the crack initiation at the support structures. The maximum principal stress criterion and the quadratic nominal stress criterion can be represented respectively as:

respectively as:

$$f = \left\{ \frac{\langle \sigma_{max} \rangle}{\sigma_{max}^0} \right\}$$

and

$$f = \left\{ \frac{\langle t_n \rangle}{t_n^0} \right\}^2 + \left\{ \frac{t_s}{t_s^0} \right\}^2 + \left\{ \frac{t_t}{t_t^0} \right\}^2$$

Here, σ_{max}^0 represents the maximum allowable principal stress, t_n^0 is the maximum allowable component normal to the likely crack surface, and t_s^0 and t_t^0 are the maximum allowable shear components on the likely crack surface. The symbol $\langle \, \rangle$ represents the Macaulay bracket with the usual interpretation. The Macaulay brackets are used to signify that a purely compressive stress state does not initiate damage. Damage is assumed to initiate when the maximum principal stress ratio or the quadratic interaction function defined in the expression above reaches a value of one [8]. In the region where the maximum principal stress criterion is specified, a crack orthogonal to the maximum principal stress direction is introduced in the enriched element when the damage initiation criterion is satisfied. In the region where the quadratic nominal stress criterion is used, the likely crack surface will be orthogonal to

the element local 2-direction when the damage initiation criterion is satisfied in the enriched element.

Once the corresponding damage initiation criterion is reached, the fracture energy based damage evolution law is then used to govern the rate at which the cohesive stiffness between the cracked element surfaces is degraded. Mixed mode power law described below is used.

$$\left\{\frac{G_n}{G_n^0}\right\}^{\alpha} + \left\{\frac{G_s}{G_s^0}\right\}^{\alpha} + \left\{\frac{G_t}{G_t^0}\right\}^{\alpha} = 1$$

Here G_n^0 is the critical fracture energy in the crack normal direction, G_s^0 and G_t^0 are the critical fracture energies in the shear directions on the crack surface, and α is the exponent. When the above condition associated with the dissipated fracture energies and their critical values is satisfied, the cohesive stiffness between the cracked element surfaces becomes zero.

Fracture energy for damage evolution is defined to 26MPa-mm [14]. The maximum allowable normal and shear components t_n^0, t_s^0 and t_t^0 are set equal to 312 MPa, 330 MPa and 350 MPa respectively. The critical fracture energies, G_n^0, G_s^0 and G_t^0 associated with the normal and the two shear modes are all set equal to 26 $MPa\text{-}mm$, and the exponent α is set equal to 1.

A small value of viscous regularization is used to overcome the severe convergence difficulties associated with the stiffness degradation on the cracked element.

6.   Experimental Validation

An experimental test is performed with identical same material and machine process settings as used in the FEA simulation using Renishaw AM400 machine having a $200W$ SPI Ytterbium fibre laser with a spot size diameter of $70\ \mu m$. The chemical composition of material IN625 [15] is shown in Table 3.

Table 3:   Chemical composition of Inconel 625 (mass %)

C	Cr	Ni	Si	Mo	Fe	Ti	Al	Nb
≤0.10	20-23	Balance	≤0.50	8-10	≤5.0	≤0.40	≤0.40	3.15-4.0

The support structure and part set up are purposefully oriented with an angle on build tray to avoid creating pressure wave while dosing new powder layer with wiper. Scan path and slicing information are generated using procedure mentioned in the earlier section. The substrate was heated to $170°C$ and process parameters are set as defined earlier in table 1 and 2. Build plate of S275/S355 material with dimension 248×248×33 mm is used. Gas flow

recirculation pump motor frequency of 36hz is utilized to achieve clean processing conditions. Total build time for printing the model is observed around 24 hours with 2603 layers. Figure 6 shows the printed turbine blade.
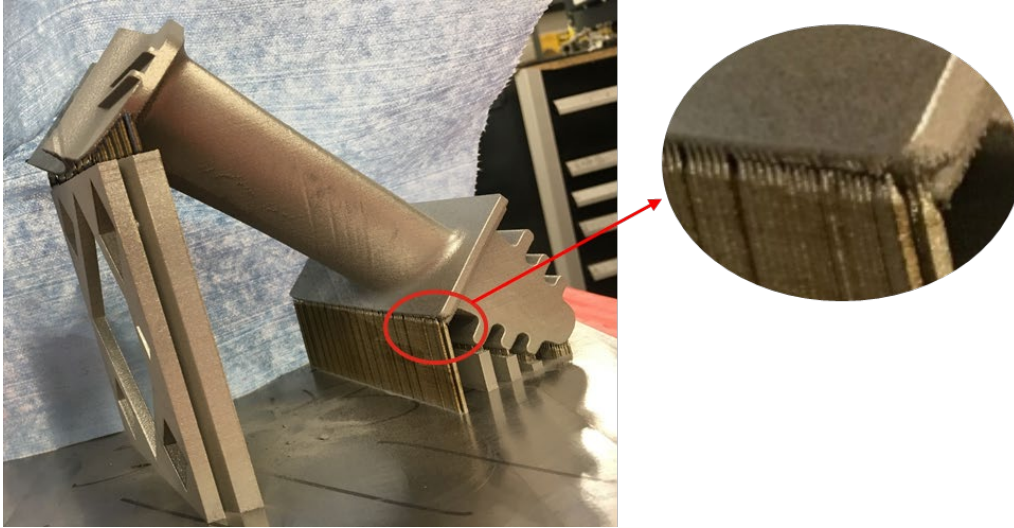

Figure 6:   Printed turbine blade

Delamination/cracking behavior is observed at the column support and part interface which was the major reason for wiper adjustment.

7.   Results and discussion

FEM displacement at the end of printing and experimental test are compared in Figure 7. Delamination/crack is observed at matching positions. This delamination has caused increased distortion at two of the four corners of the blade platform which can be observed in lighter green color in the simulation results. The enriched element is fractured when the damage initiation criterion is satisfied and crack starts to open up with residual stresses remained on the crack surfaces. The relative movements of the crack surfaces in the enriched elements are governed by the dissipated fracture energies in both the normal and the shear modes. The residual stresses on the crack surfaces eventually become zero when the dissipated fracture energies reach their critical values, leading to eventual failure in the enriched element. The maximum displacement of around 5.08mm is observed at shroud.

The success in the validation of the crack location, crack growth direction and crack length provides confidence in using FEA simulation to predict crack initiation and propagation during additive manufacturing LPBF-AM process. In some cases, such delamination can result in wiper damage and major build failures, and simulations could be used to guide proper support strategies and build planning to ensure successful build at the first time.
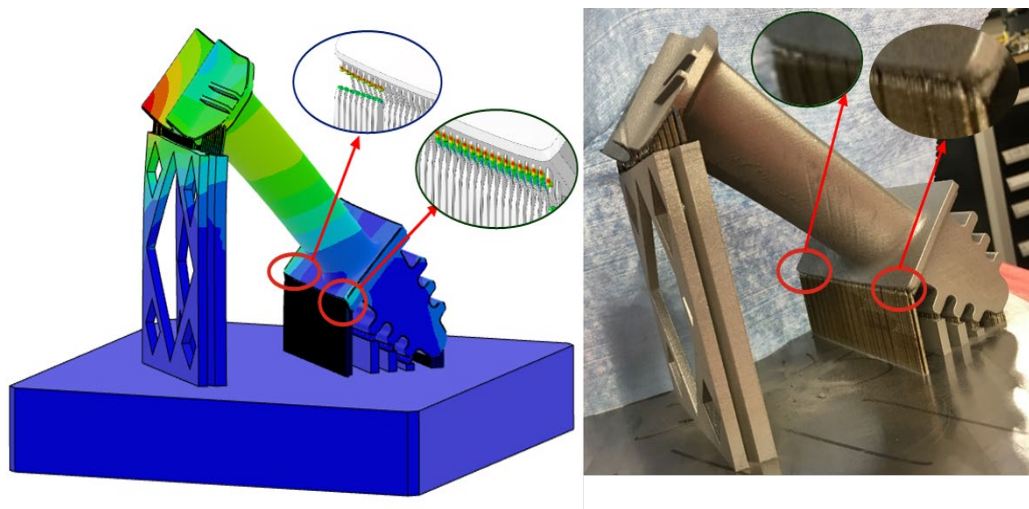
Figure 7:   Simulation and experiment results comparison

8.   Conclusion

In this paper, in-process crack modeling from LPBF-AM technology was presented. Finite element method was validated with the experimental trial as well which show good correlation between the two. Sequential thermo-mechanical analysis with extended finite element method (XFEM) was used to model crack initiation and propagation during LPBF-AM process. FEA predictions are found in good agreement with experiment because analysis utilizes actual laser path used in the LPBF-AM printer to model moving heat source, automatic computation of free evolving surfaces for convection/radiation, and correct criteria of cohesive segments method in XFEM.

Ongoing work includes changing the column supports design based on these results and modifying the orientation of the part to evenly balance the mass. In continuation of this, we are trying change turbine blade orientation and design thicker columns supports so that there will not be any crack in conical cross section at conjunctions with the part. More importantly, the proposed modeling technique can be helpful in industrial applications and can also be extended to other materials.

9.   References

[1]   C. T. Sims, N. S. Stoloff, and W. C. Hagel (1987). *Superalloys II*: Superalloys II. 615.

[2]   Das, P., Mhapsekar, K., Chowdhury, S., Samant, R., Anand, S. (2017). *Selection of build orientation for optimal support structures and minimum part errors in additive manufacturing*: Computer-Aided Design and Applications.1–13.

[3] Jingchao Jiang, Xun Xu, and d Jonathan Stringer (2018). *Support Structures for Additive Manufacturing: A Review*: Journal of manufacturing and materials processing, 2. 64.

[4] https://www.renishaw.com/en/design-for-metal-am-a-beginners-guide--42652

[5] Powder Bed Fabrication app https://help.3ds.com/2019x/English/DSDoc/DelPbfUserMap/delpbf-c-ov.htm?ContextScope=onpremise&id=4bbe56526cb54515bbe2fb404d64e336#Pg0

[6] QuantAM v5.0.0.135 2019 build preparation software. *Quick start guide H-5800-1158-03-A*.

[7] Tripathy, S., Chin C., London T., Ankalkhope U. and Oancea V. (2017). *Process Modeling and Validation of Powder Bed Metal Additive Manufacturing*: NAFEMS World Congress.

[8] Abaqus Analysis User's Guide 2018 *Modeling discontinuities as an enriched feature using the extended finite element method.*

[9] Carter L.N., Attallah M.M. and Reed R.C. (2012). *Laser powder bed fabrication of nickel-base superalloys: influence of parameters; characterization, quantification, and mitigation of cracking*: 12th International Symposium on Superalloys. 795-802.

[10] S. Suresh (1998). *Fatigue of Materials*: Cambridge University Press.

[11] Hallber Emil (2018). *Investigation of hot cracking in additive manufactured nickel-base superalloys*: Master Thesis. 1-64.

[12] Gu D.D., Hagedorn Y. and Meiners W. (2012). *Densification behavior, microstructure evolution, and wear performance of selective laser melting processed commercially pure titanium*: Acta Materialia, 60(9). 3849-3860.

[13] Abaqus Analysis User's Guide 2018. *Sequentially coupled thermal-stress analysis*

[14] Puppala G., Moitra A., Sathyanarayanan S., Kaul R., Sasikala G., Prasad R.C. and Kukreja L.M. (2014). *Evaluation of fracture toughness and impact toughness of laser rapid manufactured Inconel-625 structures and their co-relation*: Materials and Design, 59. 509-515.

[15] Renishaw data sheet (2017). *In625-0402 powder for additive manufacturing*